



13 - 16 May 2014
Putra World Trade Centre
Kuala Lumpur, Malaysia



Book of Abstracts

**International Symposium on Corrosion
& Materials Degradation**

ISCMD2014

A novelty method to determine flow accelerated corrosion and computational fluid dynamics simulation in the elbows

Muhammadu Masin Muhammadu,^a Kahar Osman^b Esah Hamzah^c

¹Department of Mechanical Engineering, Federal University of Technology, P. M. B. 65, Gidan-Kwanu, Minna, Nigeria

²Department of Thermo-fluids Engineering, Faculty of Mechanical Engineering, Universiti Teknologi Malaysia, 81310, Johor Bahru, Malaysia.

³Department of Materials and Manufacturing Engineering, Faculty of Mechanical Engineering, Universiti Teknologi Malaysia, 81310, Johor Bahru, Malaysia.

¹masin.muhammadu@futminna.edu.ng, ²kahar@fkm.utm.my, ³esah@fkm.utm.my

Corresponding Author

esah@fkm.utm.my

Abstract:

A novel method by combining array electrode technique with computational fluid dynamics (CFD) simulation was proposed to determine the correlation between the corrosion behaviour in the elbow of pipeline and the hydrodynamics of fluid flow. It is demonstrated that the distribution of the measured corrosion rates is in good accordance with the distributions of flow velocity and shear stress at the elbow. The corrosion rates at the inner wall of elbow were higher than those at the outer wall of elbow. The maximum corrosion rate appears at innermost side while the minimum corrosion rate at outermost side of the elbow. The flow accelerated corrosion (FAC) rate conforms to the experimental results in lab, which are calculated by some other FAC rate prediction models. In this paper, a new prediction model was proposed to calculate the FAC rate in the elbow, which combines the steady-state mass transfer model of electrochemical theory and one-dimensional galvanic corrosion model. The simulations were performed using the AUTODESK Simulation 2013.

Keywords: Computational fluid dynamics, elbow, fluid flow, velocity, flow accelerated corrosion

Introduction

Flow accelerated corrosion (FAC) causes wall thinning (metal thickness loss) of carbon steel piping, tubing and vessels exposed to flowing water or wet steam. Flow accelerated corrosion has caused a large number of failures in piping and equipment's in all types of fossil, industrial steam, and nuclear power plants and it is a predominant mode of failure of pipelines in the secondary circuit and has also affected carbon steel pipelines in the primary circuit of light water reactors (LWR) [1-2].

Flow accelerated corrosion is distinct from erosion-corrosion and is primarily a corrosion process aided by chemical dissolution and mass transfer. In practice, there may be some contribution from the mechanical factors that lead to removal of corroded scallops on material surface to become loose and flow out with the high velocity process fluid. This might be further accelerating the overall flow accelerated corrosion rate but would not become a factor for thinning by itself (i.e. without first the electrochemical dissolution leading to flow accelerated corrosion and formation of loosely held scallops). The corrosion rate is first determined by the rate of transfer of ionic species in between the surface and the

fluid. If the corrosion reaction is rapid and the corrosion product has low solubility in bulk fluid, the corrosion rate is governed by the concentration gradient as shown in equation (1), where CR is the corrosion rate, k is the mass transfer coefficient, C_w is the concentration of rate limiting species in the boundary layer at the metal wall, and C_B is the concentration of rate limiting species in the bulk fluid.

$$CR = k (C_w - C_B) \quad (1)$$

Flow velocities associated with flow accelerated corrosion increase this concentration gradient and thus increase the corrosion rate. No evidence of removal of the oxide film purely due to mechanical shear has been found on the flow accelerated corrosion damaged surfaces of feed water piping [3].

Many researchers have proposed some models to predict the flow accelerated corrosion rate. However, these models were based on the mass transfer theory, and the calculated results were in accordance with the laboratory experiments. For instance, in 1980, [4] predicted that model about flow accelerated corrosion rate, which assumed that when the dissoluble Fe_3O_4 met the condition of the equation of Swanton and Bases, then the flux of dissolved Fe^{2+} could be employed to express the FAC rate. This model emphasized the FAC process of electrochemical reactions and mass transfer. However, this model cannot explain the relationship between temperature and FAC rate. The proposed the MIT model [5] on the on basis to considered that the structure of the corrosion product could influence the FAC rate, and this model could explain the relationship between temperature and FAC rate. But some parameters including the thickness of oxidation film and porosity were difficult to measured in the MIT model. Therefore, the MIT model cannot be extended. Afterwards researchers paid more attention to the fluid mechanics factors of the local flow which influenced the FAC rate, and some software's of predicting the FAC rate were developed, such as CHECWORKS procedures of the electric power research (EPRI). However, [6] applied mathematics software MATLAB to predict the FAC rate; known as Fuzzy Rules.

In oil and gas transportation, elbow is an important part of most practical pipe configurations. However, the flow pattern in a 90° elbow is subject to great changes in flow direction and flow velocity [7], thus leading to significant difference in corrosion behaviour at different locations of elbow. Due to the sudden change in flow pattern, the wall thinning by FAC is exacerbated at elbow. Therefore, FAC at elbow is rather serious among the damages of pipelines [8]. Apparently, there should be correlation between the corrosion behaviour at different locations of elbow and the flow patterns. Array electrode technique, a configuration of multi-electrodes system, can be used for determining the heterogeneous electrochemical corrosion difference at different locations of elbow.

In this work, a novel model was developed to study the FAC rate and hydrodynamic effects of fluid flow on the FAC in a 90° elbow by combining array electrode technique with computational fluid dynamics (CFD) simulation. The Autodesk was used to simulate the flow field of an elbow. Then the novel model will be used to investigate the distribution of the current density of oxygen-absorbed corrosion and the current density of galvanic corrosion. The primary objectives of this work are to numerically simulate and characterize the flow patterns within a pipeline elbow, to determine the correlation between the corrosion behaviour at a pipeline elbow and the distributions of the current density of oxygen-absorbed corrosion and the current density of galvanic corrosion and shear stress.

2. Computational Fluid Dynamics (CFD) simulation

Professional fluid simulation software Fluent was employed to perform CFD simulation. Pre-processing software Autodesk 2013 was used to establish geometric model. The straight

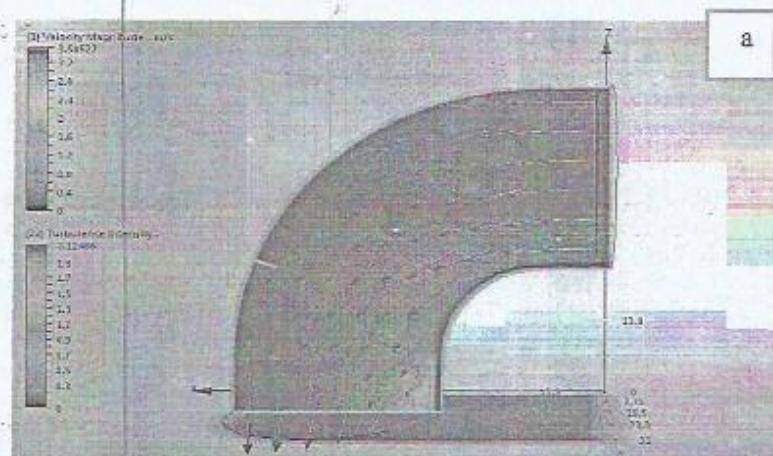
section upstream of the entrance of elbow ($\theta = 0^\circ$) was set as 1 m and the straight section downstream of the exit of elbow ($\theta = 45^\circ$) was set as 0.5 m to ensure a full-developed and stable flow condition at elbow test section. The volume meshes were constructed with the interval size of 0.004 m. A flow velocity of 2.5 m/s at the inlet and an atmospheric pressure (1.01325×10^5 Pa) at the outlet were set as the boundary conditions (see table 1). The fluid was assumed to be compressible and a $k-\epsilon$ turbulent model (double equation model) was used to numerically solve the simulation since the fluid flowed at a Reynolds number of 622313 (calculated according to the geometrical dimension of pipeline and flow velocity). The Reynolds number was much higher than 4000, indicating a turbulent flow. k , which refers to turbulent kinetic energy, was set as $1 \text{ m}^2/\text{s}^2$, and ϵ , which refers to turbulent dissipation rate, was set as $1 \text{ m}^2/\text{s}^3$. The turbulence intensity in this simulation was 10%. The $k-\epsilon$ turbulence equation was solved by iterative method with a convergence criterion of 0.000001.

Table 1: Operating parameters

Temperature (°C)	Pressure (MPa)	Flow velocity (m/s)	Material/ Fluid	Electrical conductivity ($\mu\text{S}/\text{cm}$)	Concentration of dissolved oxygen (ppm)
125	1.01325×10^5	2.5(622313)	Water	34.9	3.1

A dimensionless variable for the called the Reynolds number which is simply a ratio of the fluid dynamic forces and the fluid viscous forces, is used to determine what flow pattern will occur. The equation 2 shows the Reynolds number (R_e), where v is the fluid velocity; D is the diameter of the pipe, μ is the viscosity and ρ is the density of water respectively.

$$R_e = \frac{\rho v D}{\mu} \quad (2)$$



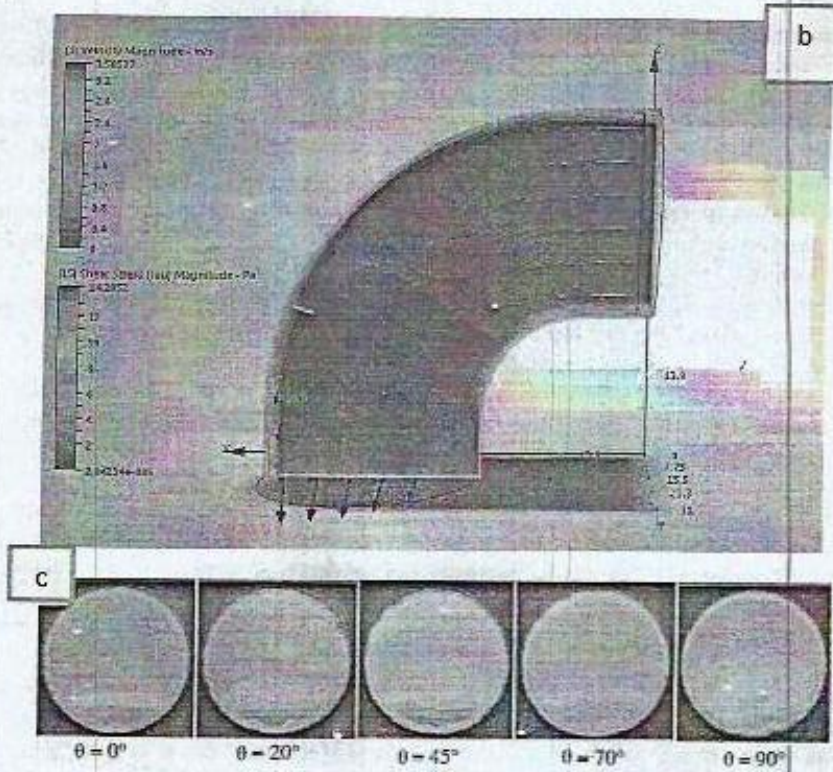


Fig. 1: Fluid flow field and shear stress distribution along the elbow by CFD simulation: (a) three-dimensional contour of velocity, (b) three-dimensional contour of shear stress, and (c) variations of flow velocity in cross-section along the elbow.

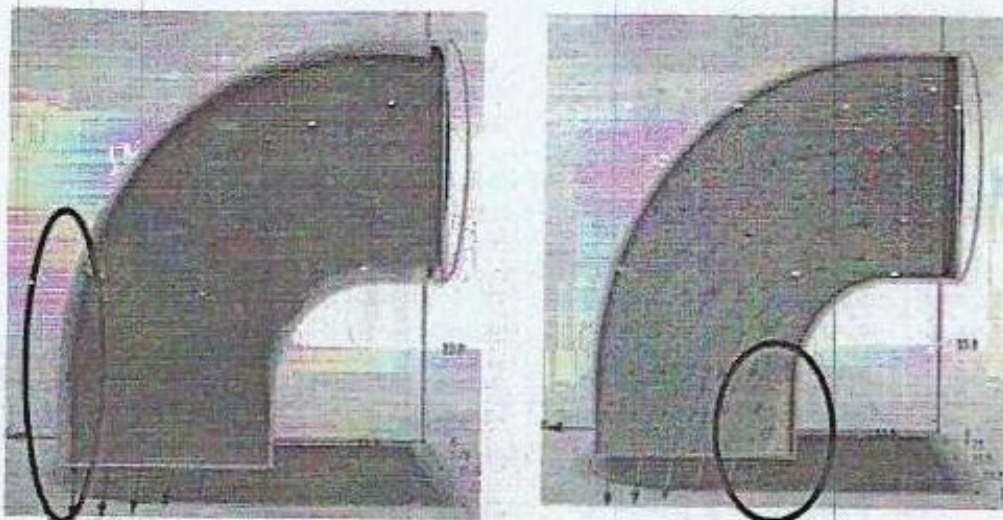


Fig.2: Predicted areas where corrosion expected occur in the elbows

3. The corrosion modelling (Algorithms)

When the fluid crosses the solid wall, the boundary layer is formed, causing larger velocity gradient near the solid wall. Due to the existence of the fluid boundary layer, mass transfer process of dissolved oxygen from the bulk of the fluid to the solid wall will be affected. In the ideal steady diffusion process, the mass transfer is mainly realized by convection. However, the mass transfer process can be divided into the convection outside the boundary layer and the diffusion inside the boundary layer, when the boundary layer comes into existence.

The Mass transfer process of dissolved oxygen is also converted from forced convection to concentration mass transfer, and this layer of the fluid is named as diffusion convection layer. When the fluid velocity is below a certain value, the mass transfer process of dissolved oxygen is controlled by the concentration of mass transfer, and this layer of fluid is called diffusion layer. Therefore, the mass flow structure is divided into three areas which are convection layer, diffusion-convection layer, and diffusion layer.

In the convection layer the velocity equals to the main velocity, therefore, the concentration of dissolved oxygen C_b equals to the concentration of saturated dissolved oxygen in the medium. In the diffusion-convection layer, mass transfer process includes concentration mass and convection mass. The mass transfer coefficient is

$$K_1 = 0.646 \left(\frac{lv^0 \rho}{\mu} \right)^{1/2} \left(\frac{\mu}{\rho D_d} \right)^{1/3} \left(\frac{D_d}{l} \right) \quad (3)$$

This is imply that K_1 is the mass transfer coefficient, l is the characteristic length of the solid wall, v^0 is the main velocity of the fluid, ρ is the density of the fluid, μ is the dynamic viscosity of the fluid, and D_d is the diffusion coefficient.

In the diffusion layer, the velocity of the fluid is close to zero. This layer of fluid is assumed to be motionless. Convection mass transfer has little influence in the area; mass transfer process is mainly achieved by concentration difference. However, [9] proposed that the diffusion coefficient of gas under the water is given by

$$D_d = (1.25V_{bA}^{-0.19} - 0.365) (10^{-8}) \mu_w^{\frac{9.59}{V_{bA}} - 1.12} T^{1.52} \quad (4)$$

Where V_{bA} is the molar volume of the oxygen, μ_w is the density of the water, and T is absolute temperaturc.

The electrochemical corrosion occurs in the duct, in which the cathode reaction and anodic reaction occur on the surface (see figure 3). When the reaction achieves equilibrium, the anode current density equals the cathodic current density, and the total current density is zero. The condensed water of pure steam pipeline, the concentration of dissolved oxygen in the fluid is very low. The corrosion reaction is mainly controlled by cathodic reaction, thus the concentration of dissolved oxygen, which diffuses from the bulk to the duct surface, can be employed to express the corrosion rate.

The calculation formula of corrosion current density

$$\text{The corrosion current density, } I_{corr} = nFK_1C_s \quad (5)$$

This implies that F is the Faraday constant, n is the electrode number of transferring in corrosion reaction and C_s is the concentration of dissolved oxygen arriving at the wall.

When the electrochemical reaction coefficients has small discrepancy with the mass transfer coefficient of dissolved oxygen, the corrosion current density I_{corr} can be expressed as

$$I_{corr} = \frac{nFK_1K_2C_b}{nFK_1 + K_1K_2\delta_0 + K_2D_d\delta_B} \quad (6)$$

This implies that K_2 is the electrochemical reaction coefficient and δ_0 is the thickness of the diffusion layer respectively.

$$\text{Where } K_2 = nFK_0 \cdot \exp\left(-\frac{n\alpha F\Delta\varphi}{RT}\right) \quad (7)$$

and

$$\delta_0 = 3\left(\frac{1}{S_c}\right)^{1/3} \cdot \delta_B \quad (8)$$

This is imply that R is the ideal gas constant, T is the absolute temperature, K_0 is the reaction coefficient, α is the balance number, $\Delta\epsilon$ is the activation energy, δ_B is the thickness of the boundary layer and C_b is the concentration of rate limiting species in the bulk fluid respectively.

However, according to the equations of the oxygen-absorbed dynamics controlled by dissolved oxygen mass transfer, the corrosion potential is expressed as

$$E_{corr} = \frac{RT}{\alpha nF} \cdot \ln\left(1 - \frac{I_{corr}}{I_d}\right) \quad (9)$$

Where I_d is equal to the limited current density, E_{corr} is equal to the corrosion potential, I_{corr} is equal to the corrosion current density and I_f is equal to the Faraday current density.

The calculation model of the flow accelerated corrosion rate is assumed as a classic model, in which calculated results were consistent with the experimental results. When the fluid flows through the elbow, fluid medium it causes centrifugal force. The core of fluid moves to the outward bend of the elbow. In the inward bend of the elbow, the magnitude of flow velocity comes to maximum, and it makes the process of mass transfer stronger. This imply that, in the outward bend of the elbow, due to the effect of centrifugal force, velocity is relatively slow, which makes the process of mass transfer weaker. According to Equation (8), the corrosion rate of the inward bend of the elbow is larger than any other places of the elbow surface; but the fact shows that corrosion perforation in the outward bend of the elbow happens earlier than in the inward bend of the elbow [9], the actual results and the calculated results are opposite. The inward bend of the elbow, which is an oxygen-enriched area, acts as the cathode of the galvanic corrosion system. The outward bend of the elbow is an oxygen-poor area, which acts as the anode of the galvanic corrosion system. The galvanic corrosion current can restrain the corrosion process of the inward bend of the elbow, and accelerate the corrosion rate of the outward bend of the elbow.

The layer was regarded as the ionic conductor of the galvanic corrosion system and the duct becomes a natural electronic conductor. The arbitrary cross-section of the elbow is simplified to a three-dimensional model (see fig. 4). The inward bend of the elbow is considered as zero in the coordinate system and the outward bend of the elbow is the point b; distance from point zero to point b equals to the arc length from point A to point B in the

distribution of the velocity magnitude. The model assumes that the thickness of ionic conductors which covers the duct wall is equal to one another.

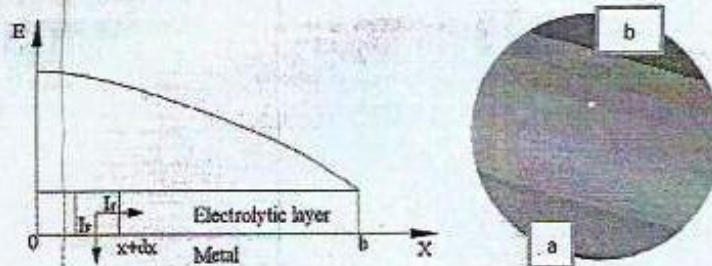


Fig. 3: Three-dimensional galvanic corrosion structure

For the galvanic corrosion system, there are Faraday current density, current density flowing, corrosion potentials of material to a reference electrode (E^X) and the potential in the ionic conduction layer (Φ). Direction of Faraday current density (I_F) is perpendicular to the surface; direction of flowing current I_f is parallel to the surface. Faraday current density means the current density which goes through the ionic conduction layer and goes into the duct surface and I_F is equal to

$$I_F = \frac{\Phi}{R_p} \quad (10)$$

Where R_p is equal to the polarization resistance of the material.

Current density flowing is a flowing in the ionic conduction layer, equation (10) becomes

$$I_F = \frac{1}{R_s} \cdot \frac{d\Phi}{dx} \quad (11)$$

Where R_s is the solution resistance and Φ is the difference between the potential of the start and end point, which constitute the galvanic corrosion system.

$$\text{But } \Phi = -(E^X - E_{corr}) \quad (12)$$

Where E^X is equal to the electrode

In the stable corrosion system, the current density system, the current density flowing into the unit and the current density flowing out of the unit ought to be equal, which is expressed as

$$I_F \cdot dx = (I_{f|x+dx} - I_{f|x}) \quad (13)$$

Substituting equation (12) into equation (13), we have

$$\frac{d^2\Phi}{dx^2} = \frac{R_s}{R_p} \theta \quad (14)$$

However, the galvanic corrosion potential is obtained by solving differential equation as

$$\Phi = A \cdot \exp(Lx) + B \cdot \exp(-Lx) \tag{15}$$

But, the boundary condition of the galvanic corrosion can be expressed as

$$\begin{cases} x = 0, \Phi = E_{corr}^b \\ x = b, \Phi = E_{corr}^b \end{cases} \tag{16}$$

Also,

$$\begin{cases} X = \frac{E_{corr}^b - E_{corr}^0 \cdot \exp(-Lb)}{\exp(Lb) - \exp(-Lb)} \\ Y = \frac{E_{corr}^b \cdot \exp(Lb) - E_{corr}^0}{\exp(Lb) - \exp(-Lb)} \\ L = \sqrt{\frac{R_s}{R_p}} \end{cases} \tag{17}$$

However, the coefficients X and Y were obtained by substituting equation (17) into equation (16) as expressed above.

4. Calculation of corrosion rate based on prediction model

The prediction model is employed to calculate the flow accelerated corrosion rate of the elbow at pipeline is categorized into the following steps, vis-a-viz:

- ❖ The computational fluid dynamics Autodcsk software 2013 was applied to get the velocity distribution in the elbow and selected the cross-section of the elbow with the maximum velocity in accordance with the velocity distribution.
- ❖ According to the velocity of the outward and inward bend of the elbow, the corrosion potential E_{corr}^0 and E_{corr}^b were obtained by using eq.(5) or eq. (6) and eq.(9) at the point A and point B. (when K_2 is greater than K_1 , the I_{corr} was calculated by eq. (5); when K_2 has little difference with K_1 , the I_{corr} was calculated using eq. (6).
- ❖ The galvanic corrosion current density i_p was calculated by using equations (18–21).

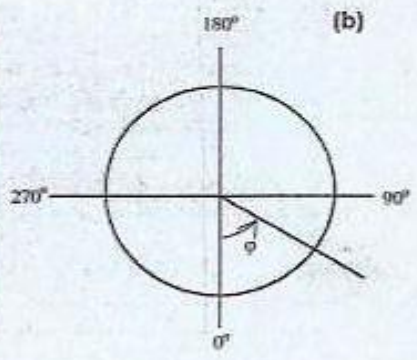
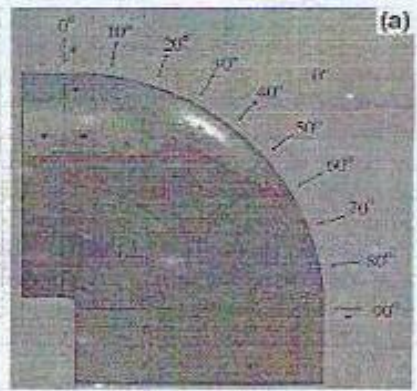


Fig.4: Variations of corrosion rate, flow velocity and shear stress along the elbow surface: (a) annotation of h , and (b) annotation of u .

The computation of the corrosion rate

The characteristics of electrochemical reaction theories and mass transfer characteristics, the corrosion control step is divided into the step of controlling electrochemical reactions and the step of controlling mass transfer. It is important to know the kind of the corrosion controlled step before calculating the corrosion rate, electrochemical reactions control or mass transfer control. In this research, the relationship between electrochemical reaction coefficient and the mass transfer coefficient to judge the electrochemical reaction steps was used. However, from equation (3), the mass transfer coefficient was calculated, and mass transfer coefficients. The k_1 was calculated to be $3.55E-5$, the electrochemical reaction coefficient $k_2 = 3.88$ was obtained from equation (7) and $\alpha = 0.4$, $k_0 = 1e-6$, $\Delta E = 0.353V$ was obtained from equation 11 respectively.

In Figure 3, the corrosion rate increases distinctly with increasing velocity from the outward bend of the elbow to the inward bend of the elbow. When the flow velocity increases, it makes the fluid boundary layer thinner, and meanwhile, it also leads to be degradation of the convection-dispersion layer. The thickness of the diffusion layer becomes thinner and mass transfer resistance becomes smaller, which causes corrosion rate to increase. The calculation results indicated that the inward bend of the elbow fails earlier than the outward bend of the elbow.

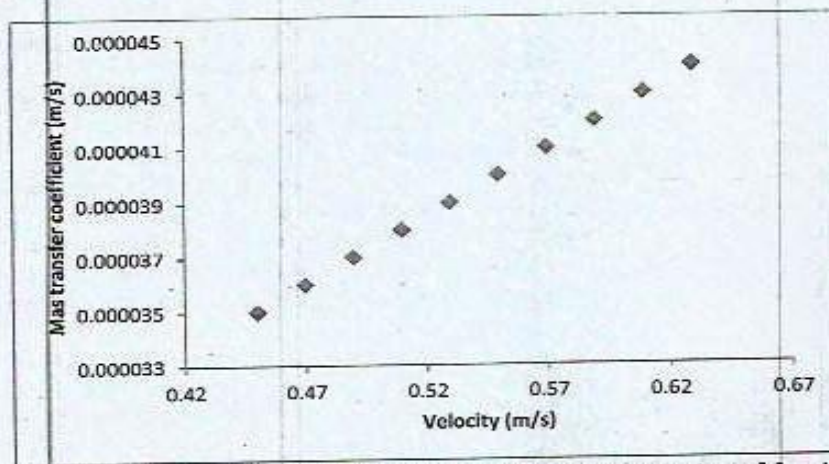


Fig.6: The distribution of the mass transfer coefficient of cross-section of $\theta = 45^\circ$

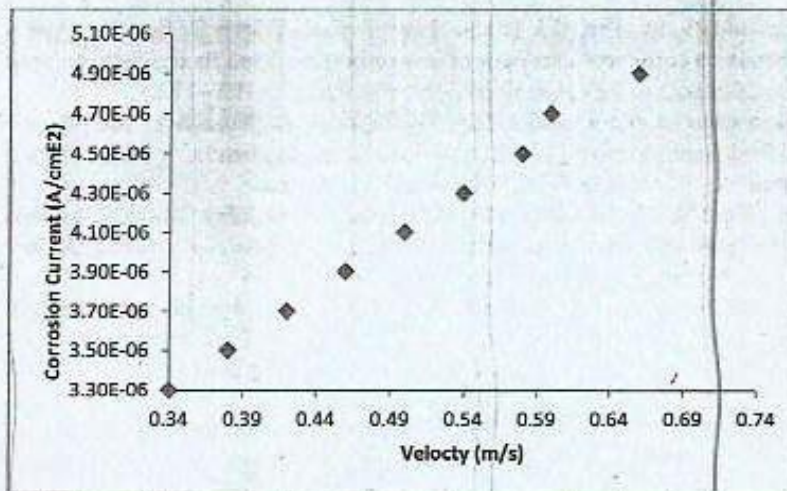


Fig.7: The distribution of the oxygen-absorbed corrosion current density of cross-section of $\theta = 45^\circ$

Calculation based on Computational Fluid Dynamics

The computational fluid dynamic software AUTO DESK was employed to calculate the elbow system, which sets up a 3D model. The mesh type was T-grid, and k-e turbulent model was used in the calculation process. Inlet boundary condition was set as velocity-inlet, and outlet boundary condition is set as pressure-outlet. SIMPLEC was adopted when calculating pressure and velocity coupling, and standard discretization is used as pressure discretization. Momentum equations, turbulent kinetic energy and turbulent kinetic energy dissipation are applied in the second-order windward discretization. The operating parameters are shown in Table 1. The symmetrical distribution of the velocity magnitude of the elbow system and the elbow cross-section of $\theta=45^\circ$ are shown in Figures 2 and 4, respectively. Figures 2 and 4 show that the flowing core shifts to the outward bend of the elbow, and the velocity of the inward bend of the elbow is greater than that of the outward bend of the elbow.

Conclusions

A novel method to determine flow accelerated corrosion with computational fluid dynamics (CFD) simulation was proposed to determine the correlation between the corrosion behaviour in the elbow of pipeline and the hydrodynamics of the fluid flow. It is demonstrated that corrosion rate in the inner wall of elbow was higher than that at the outer wall of elbow, with the higher flow velocity and shear stress at the inner wall. The maximum corrosion rate appears at innermost side of the elbow, i.e., the location with the maximum flow velocity and shear stress, while the minimum corrosion rate appears at outermost side of the elbow, the location with minimum flow velocity and shear stress. The distribution of the measured corrosion rates is in good accordance with the distributions of flow velocity and shear stress in the elbow.

The new prediction model was employed to calculate the Flow Accelerated Corrosion corrosion rate of cross-section of $\theta = 45^\circ$. Mass transfer coefficient and oxygen-absorbed corrosion current density I_{corr} increase with increasing velocity.

References

1. Muhammadu M. M., Sheriff J. M and Hamzah. E. B. Effects Of fluid flow pattern at pipe bends on corrosion behaviour of low carbon steel and its challenges, *Jurnal of Teknologi (Sciences and Engineering)* 2013, vol. 62:1, Pp 103 –112.
- [2]. Muhammadu M. M., Sheriff J. M and Hamzah. E. B., Numerical analysis of Relationship between fluid flow pattern on corrosion behaviour in pipe bends, *International Review of Mechanical Engineering*, 2014, accepted for publication.
3. Smith CL, Shah V. N, Kao T, Apostolakis G. NUREG/CR-5632: Incorporating aging effects into probabilistic risk assessment – a feasibility study utilizing reliability physics models. U. S Nuclear Regulatory Commission 2001.
4. ASM Handbook. Corrosion – fundamentals, testing and protection, vol. 13A. ASM International, the Materials Information Society, Materials Park, Ohio; 2003
- [5]. Koike M. H. Erosion–corrosion of stainless steel pipes under two-phase flow with steam quality 26%. *J Nuclear Mater* 2005; 342:125–30.
6. Shah V. N. et al. Apotolakis, NUREG/CR-5632, USNRC, Washington, DC 2001.
7. T. Shoji, Z. Lu, Y. Takeda, Y. Sato, Presented at the 14th Asia Pacific Corrosion Control Conference (APCCC), Shanghai, China, October 21–24, 2006.
8. Levich V. G. Physicochemical Hydrodynamics, Translated from the second Russian Edition. Prentice-Hall Press, New Jersey 1962.
9. Roychowdhury S, et al. Flow accelerated corrosion and control strategies in the Secondary circuit pipelines in Indian nuclear power plants. *J Nuclear Mater* 2008; 383: 86–91.
10. International Atomic Energy Agency. Material degradation and related managerial issues at nuclear power plants. In: Proceedings of technical meeting held during February 15–18, 2005 at Vienna by International Atomic Energy Agency (IAEA); 2006.
11. Shoji T, Lu Z, Takeda Y, Sato Y. Towards proactive materials degradation management in NPP – today and future. In: CD proceedings of the 14th Asia Pacific corrosion control conference (APCCC), October 21–24, 2006, Shanghai, China; 2006.